

Article

Controlled Oxidation of Cobalt Nanoparticles to Obtain Co/CoO/Co₃O₄ Composites with Different Co Content

Aleksandr S. Lozhkomoev ^{1,*}, Alexander V. Pervikov ², Sergey O. Kazantsev ^{1,3}, Konstantin V. Suliz ^{1,3}, Roman V. Veselovskiy ⁴, Andrey A. Miller ⁵ and Marat I. Lerner ^{2,3}

¹ Laboratory of Nanobioengineering, Institute of Strength Physics and Materials Science, Siberian Branch of the Russian Academy of Sciences, 634021 Tomsk, Russia; kzso@ispms.tsc.ru (S.O.K.); konstantin.suliz@gmail.com (K.V.S.)

² Laboratory of Physical Chemistry of Ultrafine Materials, Institute of Strength Physics and Materials Science, Siberian Branch of the Russian Academy of Sciences, 634021 Tomsk, Russia; pervikov@list.ru (A.V.P.); lerner@ispms.tsc.ru (M.I.L.)

³ Research and Education Center of Additive Technologies, National Research Tomsk State University, 634050 Tomsk, Russia

⁴ Schmidt Institute of Physics of the Earth, Russian Academy of Sciences, 123242 Moscow, Russia; roman.veselovskiy@ya.ru

⁵ Shared Use Center “Nanotech”, Institute of Strength Physics and Materials Science, Siberian Branch of the Russian Academy of Sciences, 634021 Tomsk, Russia; miller@ispms.ru

* Correspondence: asl@ispms.tsc.ru



Citation: Lozhkomoev, A.S.; Pervikov, A.V.; Kazantsev, S.O.; Suliz, K.V.; Veselovskiy, R.V.; Miller, A.A.; Lerner, M.I. Controlled Oxidation of Cobalt Nanoparticles to Obtain Co/CoO/Co₃O₄ Composites with Different Co Content. *Nanomaterials* **2022**, *12*, 2523. <https://doi.org/10.3390/nano12152523>

Academic Editor: Sheng Yun Wu

Received: 20 June 2022

Accepted: 20 July 2022

Published: 22 July 2022

Publisher’s Note: MDPI stays neutral with regard to jurisdictional claims in published maps and institutional affiliations.



Copyright: © 2022 by the authors. Licensee MDPI, Basel, Switzerland. This article is an open access article distributed under the terms and conditions of the Creative Commons Attribution (CC BY) license (<https://creativecommons.org/licenses/by/4.0/>).

1. Introduction

Cobalt is a transition metal that has a beneficial effect on human health [1,2]. It is contained in vitamin B12 which is beneficial in the treatment of anaemia since it provokes the formation of red blood cells [2]. Cobalt has unique magnetic, optical, electrical, and catalytic characteristics which make it suitable for a wide range of applications in the field of nanoelectronics and nanosensors [3–5].

Co₃O₄ is a multifunctional material and has many applications, such as biomedical applications [6], gas sensors [7], solar selective absorbers [8], anode materials in lithium-ion batteries [9], energy storage [10], field emission materials [11], heterogeneous catalysis [12] and others.

CoO is successfully used in catalytic processes of CO₂ hydrogenation [12], as photo- and electrocatalytic materials [13,14].

The unique properties of cobalt and its oxides are also used in Co/CoO, Co/Co₃O₄ and CoO/Co₃O₄ systems [15–20]. Such composite nanoparticles are obtained by chemical methods based on the oxidation of organometallic precursors [21,22], using solvothermal methods [23], oxidation of Co nanoparticles with water [24], and green chemistry methods [25,26].

Controlled oxidation of Co nanoparticles with oxygen during heating can become a promising method for the production of composite nanoparticles based on cobalt and its

oxides. As shown in [27], cobalt nanoparticles heated in the air form an amorphous CoO layer on the surface, which grows over time through an indirect mechanism of exchange followed by oxidation to Co_3O_4 .

Controlled oxidation of cobalt nanoparticles can contribute to the production of composites based on cobalt and cobalt oxides with a given component ratio. This is important both in terms of the evaluation of the magnetic characteristics, for example, to ensure the exchange anisotropy of the nanoparticles at the ferromagnetic/antiferromagnetic interface [28], and in terms of catalytic activity [24,29,30].

As a precursor for obtaining such composites, cobalt nanopowder obtained by electrical explosion of cobalt wire in an inert medium is promising [31]. The method is quite productive, one setup provides productivity up to 200 g/hour [32]. The purity of the product is determined by the composition of the initial wire and buffer gas of the inert medium.

The preparation of the cobalt compound and cobalt-oxide-based composites using Co nanopowders has not been considered. In this regard, the purpose of this paper is to study the patterns of oxidation with air oxygen by heating Co nanoparticles obtained by electrical explosion of wire and to determine the effect of temperature on the composition, morphology and magnetic properties of oxidation products.

2. Materials and Methods

Co nanoparticles were obtained using a setup described in [33] at electrical explosions of cobalt wire (chemical purity of 99.98%) with a diameter of 0.5 mm in argon (chemical purity of 99.993%), at a voltage of 29 kV and a capacity of 3.2 μF . The electrical schematic of the setup and the current and voltage recording are given in [34].

The morphology of nanoparticles was studied by transmission electron microscopy (TEM) using a JEM-2100 microscope (JEOL, Tokyo, Japan). The average size of nanoparticles was determined by particle size distribution histograms obtained from electron microscopy data. To construct a histogram, 2842 particle diameters were measured. The average size was determined by the expression $a_n = \Sigma n_i a_i / \Sigma n_i$, where n_i is the number of particles that fell into the selected size range, a_i is the average diameter of the particles in the selected interval.

Oxidation of Co nanoparticles was studied by methods of thermogravimetric analysis and differential scanning calorimetry (TG-DSC) using NETZSCH STA 449F3 (Netzsch, Waldkraiburg, Germany). For this, 5 mg samples were heated in airflow from ambient temperature to 760 °C at a heating rate of 10 °C/min.

Composite nanoparticles were obtained by heating the Co nanopowder in a muffle furnace up to a range of temperatures (150, 250, 300, 450 or 600 °C) at a heating rate of 10 °C/min, kept for 2 h and cooled to room temperature.

The phase composition of nanoparticles was determined using a Shimadzu XRD 6000 X-ray diffractometer (Shimadzu, Kyoto, Japan). The obtained data were processed with Powder Cell 2.4 software (W. Kraus & G. Nolze, Berlin, Germany).

Magnetic properties of nanoparticles were studied at the Centre for Collective Use of the IPE RAS [35] using a PMC MicroMag 3900 vibrating sample magnetometer (Lake Shore Cryotronics, Westerville, OH, USA) at room temperature in air. Parameters of the hysteresis loop, such as coercive force (H_c), residual saturation magnetisation (M_r), and saturation magnetisation (M_s), were measured when the sample was magnetised in a magnetic field up to 15,000 E.

3. Results and Discussion

Co nanoparticles obtained by electrical explosion of wire are spherical nanoparticles with an average size of 56 nm, which are covered with a solid oxide film with a thickness of about 2.5 nm, formed as a result of passivation of nanoparticles in air (Figure 1a–c). The peaks on the diffraction pattern (Figure 1d) correspond to planes (111), (200) and (220) in accordance with a powder diffraction file of the International Centre for Diffraction Data (ICDD), card No. 00-015-0806.

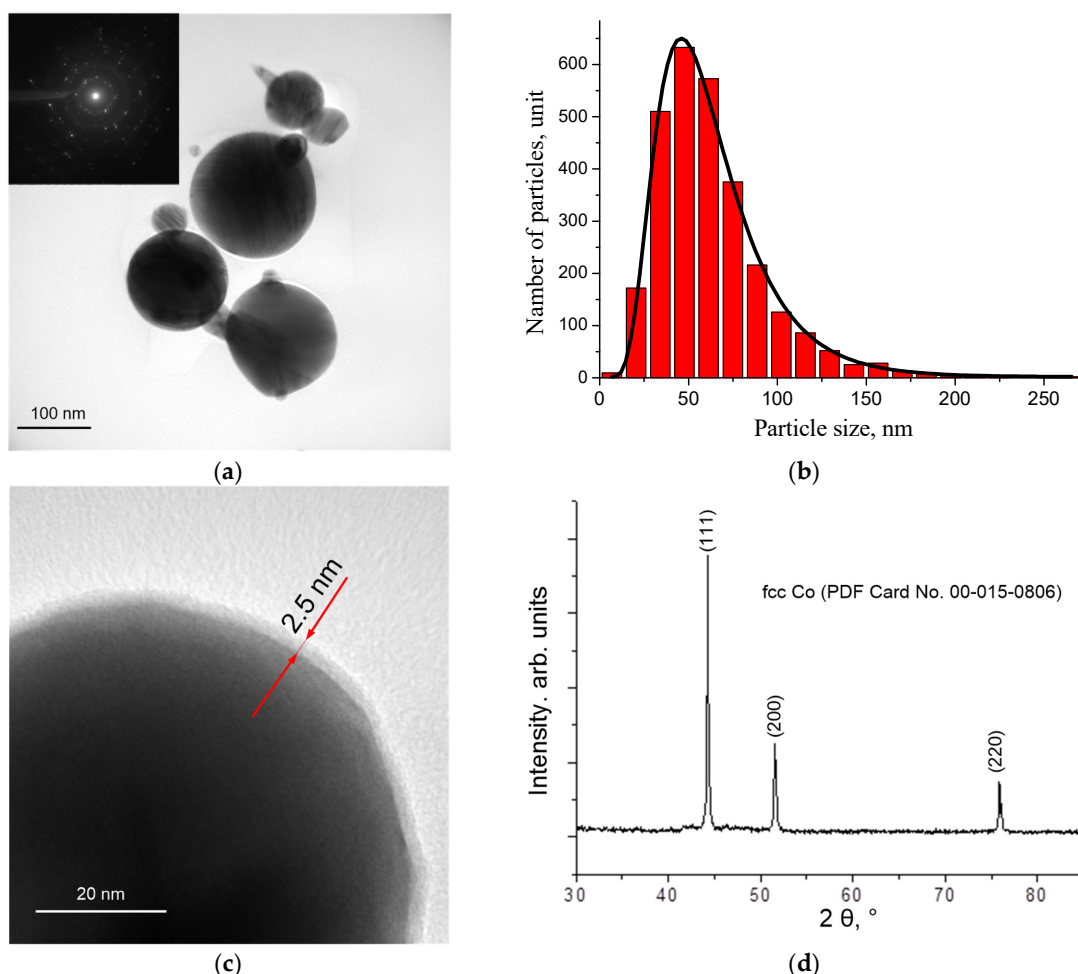


Figure 1. TEM image of cobalt nanoparticles (a), particle size distribution (b), TEM image of cobalt nanoparticles coated with oxide film (c) and X-ray phase analysis data (d).

It is known that Co is well oxidised by oxygen when heated, making it possible to produce composites based on cobalt and its oxides with different contents of components. The analysis of DSC-TG curves presented in Figure 2 shows that oxidation of nanoparticles begins at the temperature of 165 °C, accompanied by an increase of the sample mass observed on the thermogravimetric curve and the beginning of an exothermic oxidation reaction. In comparison with bulk cobalt with an oxidation temperature of about 300 °C, oxidation of nanoparticles occurs at a much lower temperature. The maximum rate of the oxidation reaction is reached at a temperature of 303 °C at which a peak is recorded on the DSC curve due to the exothermic oxidation reaction. Further heating is also accompanied by an increase in the sample mass and the appearance of another endothermic peak at 462 °C, which may be associated with the oxidation of CoO to Co₃O₄. A noticeable decrease in the oxidation rate observed by a decreasing slope of the TGA curve occurs at 550 °C. The reduced rate asymptotically approaches the constant value towards the higher temperatures, indicating the complete oxidation of the sample. The increase of sample mass was 31.9%, which is slightly lower than a theoretical weight increase of 36.2% for completely pure metal. It may be associated with the presence of cobalt oxide in the initial sample in the form of the film on the surface of nanoparticles, which can reach ~10 vol.% at an oxide film thickness of 2.5 nm.

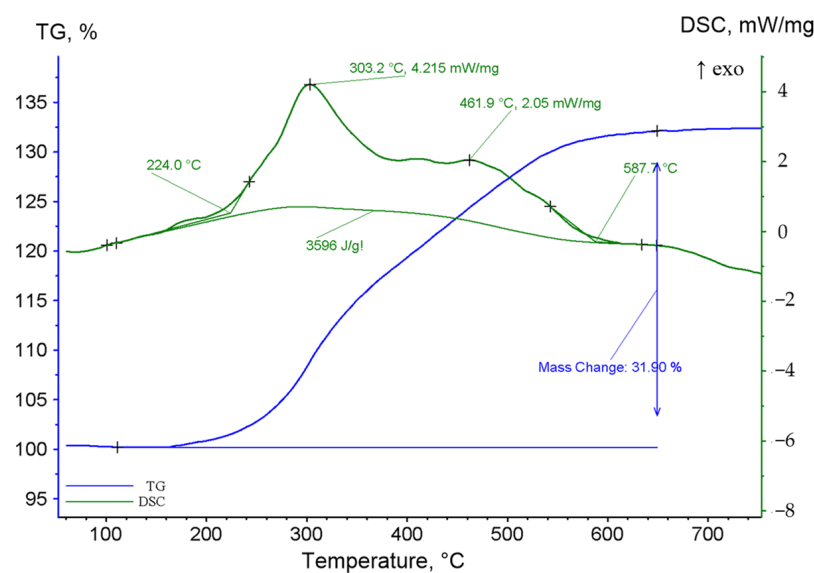


Figure 2. DSC-TG curves of cobalt nanoparticles when heated in an oxygen-containing atmosphere.

According to the X-ray phase analysis (Figure 3a), Co nanoparticles (ICDD PDF card No. 00-015-0806) are not oxidised at a temperature of 150 °C; there are no peaks corresponding to cobalt oxides on the diffraction pattern of the sample. Even after heating up to 250 °C, the peaks characteristic for CoO (ICDD PDF card No. 00-048-1719) and Co₃O₄ (ICDD PDF card No. 00-043-1003) oxides are determined in the samples in addition to the Co peaks. Further heating leads to a decrease in the intensity of the Co peaks in relation to oxides. Complete oxidation of the metal occurs at 600 °C. CoO is also oxidised to Co₃O₄ at this temperature. Quantitative X-ray phase analysis indicates exponential oxidation of the metal (Figure 3b, Table 1), which may be attributed to the diffusion limitations arising from the growing thickness of the oxide layer on the surface of the reacting particles.

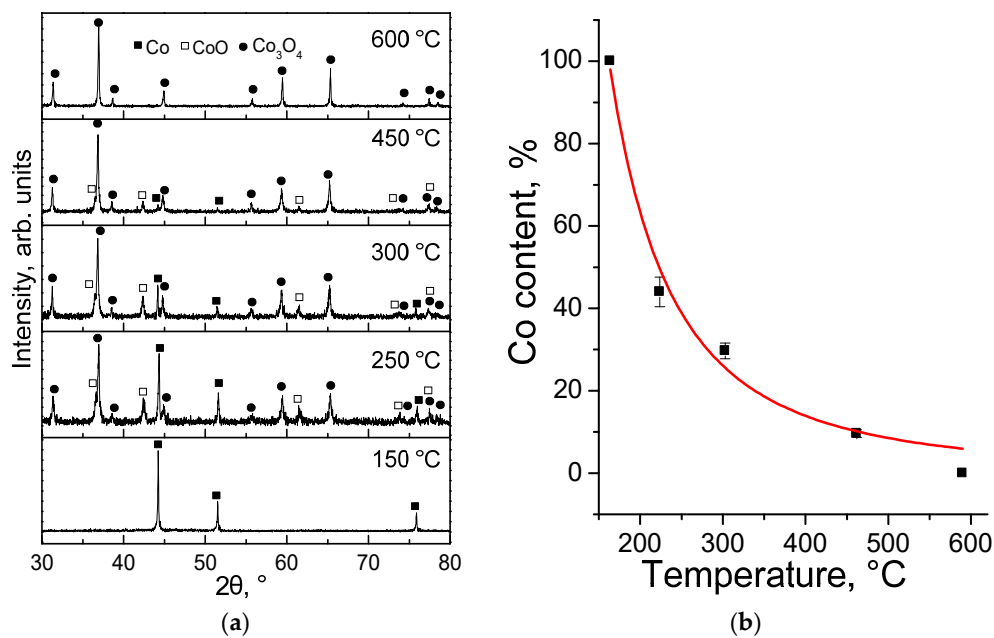


Figure 3. X-ray pattern of cobalt nanoparticles after heating at different temperatures in the air atmosphere (a) and change in the Co content in the samples depending on the calcination temperature (b).

Table 1. Quantitative assessment of the content of phases in samples according to X-ray phase analysis.

Sample	The Amount of Substance in the Samples, %		
	Co	CoO	Co ₃ O ₄
Co	100	0	0
Co/CoO/Co ₃ O ₄ (250 °C)	44.0 ± 3.6	14.7 ± 1.1	41.3 ± 2.9
Co/CoO/Co ₃ O ₄ (300 °C)	27.9 ± 1.9	12.1 ± 0.8	60.0 ± 4.2
Co/CoO/Co ₃ O ₄ (450 °C)	9.6 ± 0.9	10.2 ± 0.6	80.2 ± 4.4
Co ₃ O ₄	0	0	100

The morphology of Co particles undergoes significant changes after heating to 250 °C (Figure 4). Voids, which are typical for metals oxidised by air oxygen during heating, are formed in the particles at the metal/oxide interface—the so-called Kirkendall effect [36–38]. An increase in the heating temperature leads to the gradual removal of the metal from cavities in the formed particles and the sintering of particle fragments with the formation of ~100 nm crystallites (Figure 4). The formation of hollow cobalt particles is considered in detail in [38]. The formation of such morphology is caused by thermally activated diffusion of cobalt cations through the oxide layer, followed by oxidation.

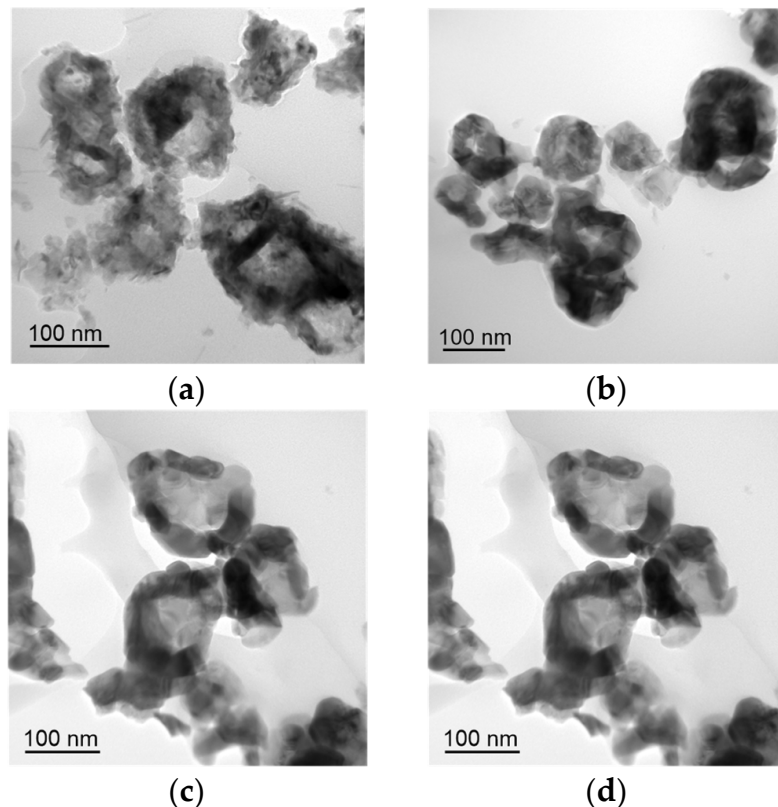


Figure 4. TEM images of the nanoparticles obtained after heating Co nanoparticles up to 250 °C (a), 300 °C (b), 450 °C (c), and 600 °C (d).

As the content of metallic cobalt in the samples decreases, their magnetic characteristics decrease (Figure 5). Cobalt nanoparticles have the highest saturation magnetisation (Ms), which was 90 emu/g. With an increase in the content of cobalt oxides in the samples, Ms decreases to 1.1 emu/g. Residual magnetisation (Mr) also decreases from 64 emu/g to 0.1 emu/g. Coercive force (Hc) decreases from 225 Oe to 51 Oe (Table 2).

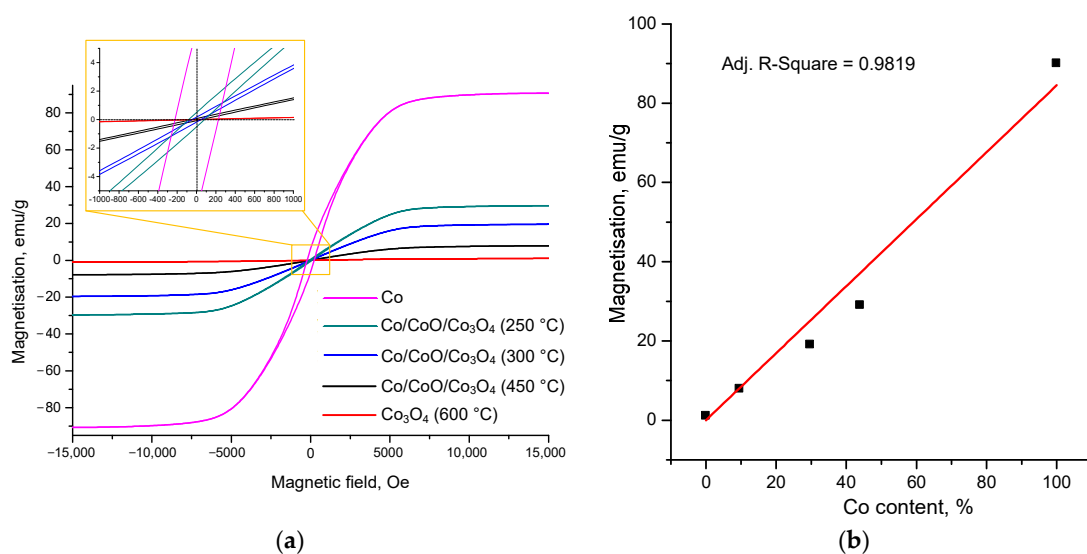


Figure 5. The dependence of saturation magnetisation of Co, Co/CoO/Co₃O₄ and Co₃O₄ nanoparticles on the magnetic field strength (a) and dependence of saturation magnetisation on the Co content in nanoparticles (b).

Table 2. Magnetic characteristics of the samples obtained.

Sample	H _c , Oe	M _s , emu/g	M _r , emu/g
Co	225 ± 11.1	90 ± 3.6	64 ± 3.4
Co/CoO/Co ₃ O ₄ (250 °C)	81 ± 5.9	29 ± 2.3	5 ± 3.4
Co/CoO/Co ₃ O ₄ (300 °C)	45 ± 3.2	19 ± 2.1	1.7 ± 3.4
Co/CoO/Co ₃ O ₄ (450 °C)	54 ± 2.9	7.9 ± 0.7	0.8 ± 3.4
Co ₃ O ₄	51 ± 2.7	1.1 ± 0.1	0.1 ± 3.4

The obtained samples exhibit the properties of magnetically soft materials, which is due to a narrow hysteresis loop and small coercive force at 25 °C (Figure 5a). The dependence of saturation magnetisation on the cobalt content in the samples can be described by a direct dependence (Figure 5b).

Thus, controlled heating of Co nanoparticles can be used to obtain composite Co/CoO/Co₃O₄ nanoparticles with similar morphology, different component contents and magnetic characteristics. According to the literature data, the magnetic characteristics of nanoparticles based on cobalt and its oxides are very different, which depends on composition, morphology, particle size and presence of impurities (Table 3). In most cases, the characteristics of nanoparticles based on Co and its oxides cannot be varied due to process parameters. In this context, the proposed method is quite attractive.

Table 3. Magnetic characteristics of composites based on cobalt compounds.

Composition of Particles	H _c , Oe	M _s , emu/g	M _r , emu/g	Reference
Co/CoO	600.5	115.5	-	[15]
CoO/Co ₃ O ₄	0.2734	3.450	85.032	[20]
Co/Co ₃ O ₄	373	127.8	-	[21]
Co/CoO	-	18	-	[22]
Co/Co ₃ O ₄	-	59.8	-	[39]
Co/CoO	-	34.6	-	[39]
Co/Co ₃ O ₄	46.9	67.7	-	[40]
Co/CoO	-	100.6–74.6	-	[41]
Co/CoO/Co ₃ O ₄	198.3–327.3	67.0–24.7	-	[42]
CoO/Co ₃ O ₄	330.8	5.8	-	[42]
Co/CoO/Co ₃ O ₄	81–54	29–7.9	5–0.8	In this work

4. Conclusions

In the study, Co nanoparticles with a face-centred cubic crystal system and an average particle size of 56 nm were obtained by electrical explosion of wire. It was established that, when nanoparticles are heated in the air, gradual oxidation of cobalt occurs with the release of heat and the formation of CoO and Co_3O_4 . This makes it possible to vary the ratio of metal and oxides in resulting composite $\text{Co}/\text{CoO}/\text{Co}_3\text{O}_4$ particles. Complete oxidation of Co nanoparticles occurs at 600 °C. $\text{Co}/\text{CoO}/\text{Co}_3\text{O}_4$ particles have a hollow structure attributed to the diffusion of cobalt into an oxide shell during heating. It was shown that the dependence of the saturation magnetisation of nanoparticles on the Co content is a linear dependence with a high degree of correlation. As the Co content decreases in nanoparticles, saturation magnetisation decreases from 90 emu/g at 100% Co content to 7.9 emu/g at 9.6% Co content and to 1.1 emu/g with complete metal oxidation.

The results obtained are important for technologies using such cobalt-based composites, as they allow varying the component ratio and provide multiple interfaces that determine the efficiency of such composites in photochemical, electrochemical, catalytic, and other processes.

Author Contributions: Conceptualization, A.S.L. and M.I.L.; methodology, A.S.L., A.V.P. and S.O.K.; software, A.V.P.; validation, A.S.L., A.V.P.; formal analysis, R.V.V., S.O.K.; investigation, R.V.V., S.O.K., A.A.M. and K.V.S.; resources, R.V.V. and A.A.M.; data curation, A.S.L. and M.I.L.; writing—original draft preparation, A.S.L., S.O.K. and A.V.P.; writing—review and editing, A.S.L.; visualization, A.S.L. and S.O.K.; supervision, A.S.L.; project administration, M.I.L.; funding acquisition, M.I.L. All authors have read and agreed to the published version of the manuscript.

Funding: The study is financially supported by the Russian Science Foundation (grant No. 21-79-30006).

Institutional Review Board Statement: Not applicable.

Informed Consent Statement: Not applicable.

Data Availability Statement: All data generated or analyzed during this study are included in this published article.

Conflicts of Interest: The authors have no conflict of interest to declare.

References

1. Faucon, M.P.; Pourret, O.; Lange, B. Element case studies: Cobalt and copper. In *Agromining: Farming for Metals*; Springer: Cham, Switzerland, 2018; pp. 233–239.
2. Iravani, S.; Varma, R.S. Sustainable synthesis of cobalt and cobalt oxide nanoparticles and their catalytic and biomedical applications. *Green Chem.* **2020**, *22*, 2643–2661. [[CrossRef](#)]
3. Egorova, K.S.; Ananikov, V.P. Toxicity of Metal Compounds: Knowledge and Myths. *Organometallics* **2017**, *36*, 4071–4090. [[CrossRef](#)]
4. Xu, Q.; Li, W.; Ding, L.; Yang, W.; Xiao, H.; Ong, W.-J. Function-driven engineering of 1D carbon nanotubes and 0D carbon dots: Mechanism, properties and applications. *Nanoscale* **2018**, *11*, 1475–1504. [[CrossRef](#)] [[PubMed](#)]
5. Ansari, S.; Bhor, R.; Pai, K.; Sen, D.; Mazumder, S.; Ghosh, K.; Kolekar, Y.; Ramana, C. Cobalt nanoparticles for biomedical applications: Facile synthesis, physicochemical characterization, cytotoxicity behavior and biocompatibility. *Appl. Surf. Sci.* **2017**, *414*, 171–187. [[CrossRef](#)]
6. Waris, A.; Din, M.; Ali, A.; Afridi, S.; Baset, A.; Khan, A.U.; Ali, M. Green fabrication of Co and Co_3O_4 nanoparticles and their biomedical applications: A review. *Open Life Sci.* **2021**, *16*, 14–30. [[CrossRef](#)]
7. Li, W.; Jung, H.; Hoa, N.D.; Kim, D.; Hong, S.-K.; Kim, H. Nanocomposite of cobalt oxide nanocrystals and single-walled carbon nanotubes for a gas sensor application. *Sens. Actuators B Chem.* **2010**, *150*, 160–166. [[CrossRef](#)]
8. Avila, A.G.; Barrera, E.C.; Huerta, L.A.; Muhl, S. Cobalt oxide films for solar selective surfaces, obtained by spray pyrolysis. *Sol. Energy Mater. Sol. Cells* **2004**, *82*, 269–278. [[CrossRef](#)]
9. Li, W.Y.; Xu, L.N.; Chen, J. Co_3O_4 Nanomaterials in Lithium-Ion Batteries and Gas Sensors. *Adv. Funct. Mater.* **2005**, *15*, 851–857. [[CrossRef](#)]
10. Kumar, R.; Kim, H.J.; Park, S.; Srivastava, A.; Oh, I.K. Graphene-wrapped and cobalt oxide-intercalated hybrid for extremely durable super-capacitor with ultrahigh energy and power densities. *Carbon* **2014**, *79*, 192–202. [[CrossRef](#)]
11. Baby, T.T.; Sundara, R. A facile synthesis and field emission property investigation of Co_3O_4 nanoparticles decorated graphene. *Mater. Chem. Phys.* **2012**, *135*, 623–627. [[CrossRef](#)]

12. Adekunle, A.S.; Oyekunle, J.A.; Durosini, L.M.; Oluwafemi, O.S.; Olayanju, D.S.; Akinola, A.S.; Obisesan, O.R.; Akinyele, O.F.; Ajayeoba, T.A. Potential of cobalt and cobalt oxide nanoparticles as nanocatalyst towards dyes degradation in wastewater. *Nano-Struct. Nano-Objects* **2019**, *21*, 100405. [[CrossRef](#)]
13. Have, I.C.T.; Kromwijk, J.J.G.; Monai, M.; Ferri, D.; Sterk, E.B.; Meirer, F.; Weckhuysen, B.M. Uncovering the reaction mechanism behind CoO as active phase for CO₂ hydrogenation. *Nat. Commun.* **2022**, *13*, 324. [[CrossRef](#)]
14. Liao, L.; Zhang, Q.; Su, Z.; Zhao, Z.; Wang, Y.; Li, Y.; Lu, X.; Wei, D.; Feng, G.; Yu, Q.; et al. Efficient solar water-splitting using a nanocrystalline CoO photocatalyst. *Nat. Nanotechnol.* **2013**, *9*, 69–73. [[CrossRef](#)]
15. Ling, T.; Yan, D.Y.; Wang, H.; Jiao, Y.; Hu, Z.; Zheng, Y.; Zheng, L.; Mao, J.; Liu, H.; Du, X.W.; et al. Activating cobalt (II) oxide nanorods for efficient electrocatalysis by strain engineering. *Nat. Commun.* **2017**, *8*, 1509. [[CrossRef](#)]
16. Liu, T.; Pang, Y.; Zhu, M.; Kobayashi, S. Microporous Co@CoO nanoparticles with superior microwave absorption properties. *Nanoscale* **2014**, *6*, 2447–2454. [[CrossRef](#)]
17. Peng, D.L.; Sumiyama, K.; Hihara, T.; Yamamuro, S.; Konno, T.J. Magnetic properties of monodispersed Co/CoO clusters. *Phys. Rev. B* **2000**, *61*, 3103–3109. [[CrossRef](#)]
18. Yan, X.; Tian, L.; He, M.; Chen, X. Three-Dimensional Crystalline/Amorphous Co/Co₃O₄ Core/Shell Nanosheets as Efficient Electrocatalysts for the Hydrogen Evolution Reaction. *Nano Lett.* **2015**, *15*, 6015–6021. [[CrossRef](#)]
19. Zhang, J.; Fu, J.; Zhang, J.; Ma, H.; He, Y.; Li, F.; Xie, E.; Xue, D.; Zhang, H.; Peng, Y. Co@Co₃O₄ Core–Shell Three-Dimensional Nano-Network for High-Performance Electrochemical Energy Storage. *Small* **2014**, *10*, 2618–2624. [[CrossRef](#)]
20. Al-Senani, G.M.; Deraz, N.M.; Abd-Elkader, O.H. Magnetic and characterization studies of CoO/Co₃O₄ nanocomposite. *Processes* **2020**, *8*, 844. [[CrossRef](#)]
21. Yousefi, S.R.; Alshamsi, H.A.; Amiri, O.; Salavati-Niasari, M. Synthesis, characterization and application of Co/Co₃O₄ nanocomposites as an effective photocatalyst for discoloration of organic dye contaminants in wastewater and antibacterial properties. *J. Mol. Liq.* **2021**, *337*, 116405. [[CrossRef](#)]
22. Verelst, M.; Ely, T.O.; Amiens, C.; Snoeck, E.; Lecante, P.; Mosset, A.; Respaud, M.; Broto, J.M.; Chaudret, B. Synthesis and Characterization of CoO, Co₃O₄, and Mixed Co/CoO Nanoparticles. *Chem. Mater.* **1999**, *11*, 2702–2708. [[CrossRef](#)]
23. Pang, M.; Long, G.; Jiang, S.; Ji, Y.; Han, W.; Wang, B.; Liu, X.; Xi, Y.; Wang, D.; Xu, F. Ethanol-assisted solvothermal synthesis of porous nanostructured cobalt oxides (CoO/Co₃O₄) for high-performance supercapacitors. *Chem. Eng. J.* **2015**, *280*, 377–384. [[CrossRef](#)]
24. Wang, D.; Guo, J.; Hu, D.; Xu, Q.; Zhang, L.; Wang, J. Co@Co₃O₄ Prepared in Situ from Metallic Co as an Efficient Semiconductor Catalyst for Photocatalytic Water Oxidation. *ACS Sustain. Chem. Eng.* **2018**, *6*, 8300–8307. [[CrossRef](#)]
25. Şahan, H.; Göktepe, H.; Yıldız, S.; Çaymaz, C.; Papat, Ş. A novel and green synthesis of mixed phase CoO@Co₃O₄@C anode material for lithium ion batteries. *Ionics* **2019**, *25*, 447–455. [[CrossRef](#)]
26. Raveau, B.; Seikh, M.M. Charge ordering in cobalt oxides: Impact on structure, magnetic and transport properties. *Z. Anorg. Allg. Chem.* **2015**, *641*, 1385–1394. [[CrossRef](#)]
27. Ha, D.-H.; Moreau, L.M.; Honrao, S.; Hennig, R.G.; Robinson, R.D. The Oxidation of Cobalt Nanoparticles into Kirkendall-Hollowed CoO and Co₃O₄: The Diffusion Mechanisms and Atomic Structural Transformations. *J. Phys. Chem. C* **2013**, *117*, 14303–14312. [[CrossRef](#)]
28. Wiedwald, U.; Lindner, J.; Spasova, M.; Frait, Z.; Farle, M. Effect of an oxidic overlayer on the magnetism of Co nanoparticles. *Phase Transit.* **2005**, *78*, 85–104. [[CrossRef](#)]
29. Xiang, S.; Dong, L.; Wang, Z.Q.; Han, X.; Daemen, L.L.; Li, J.; Cheng, Y.; Guo, Y.; Liu, X.; Hu, Y.; et al. A unique Co@CoO catalyst for hydro-genolysis of biomass-derived 5-hydroxymethylfurfural to 2, 5-dimethylfuran. *Nat. Commun.* **2022**, *13*, 3657. [[CrossRef](#)] [[PubMed](#)]
30. Feng, L.; Li, Y.; Sun, L.; Mi, H.; Ren, X.; Zhang, P. Heterostructured CoO-Co₃O₄ nanoparticles anchored on nitro-gen-doped hollow carbon spheres as cathode catalysts for Li-O₂ batteries. *Nanoscale* **2019**, *11*, 14769–14776. [[CrossRef](#)] [[PubMed](#)]
31. Yilmaz, F.; Lee, D.-J.; Song, J.-W.; Hong, H.-S.; Son, H.-T.; Yoon, J.-S.; Hong, S.-J. Fabrication of cobalt nano-particles by pulsed wire evaporation method in nitrogen atmosphere. *Powder Technol.* **2013**, *235*, 1047–1052. [[CrossRef](#)]
32. Kotov, Y.A. Electric Explosion of Wires as a Method for Preparation of Nanopowders. *J. Nanoparticle Res.* **2003**, *5*, 539–550. [[CrossRef](#)]
33. Lerner, M.I.; Glazkova, E.A.; Lozhkomoev, A.S.; Svarovskaya, N.V.; Bakina, O.V.; Pervikov, A.V.; Psakhie, S.G. Synthesis of Al nanoparticles and Al/AlN composite nanoparticles by electrical explosion of aluminum wires in argon and nitrogen. *Powder Technol.* **2016**, *295*, 307–314. [[CrossRef](#)]
34. Pervikov, A.V. Structural and phase transformations in zinc and brass wires under heating with high-density current pulse. *Phys. Plasmas* **2016**, *23*, 060701. [[CrossRef](#)]
35. Veselovskiy, R.V.; Dubinya, N.V.; Ponomarev, A.V.; Fokin, I.V.; Patonin, A.V.; Pasenko, A.M.; Fetisova, A.M.; Matveev, M.A.; Afinogenova, N.A.; Rud'Ko, D.V.; et al. Shared Research Facilities “Petrophysics, Geomechanics and Paleomagnetism” of the Schmidt Institute of Physics of the Earth Ras. *Geodyn. Tectonophys.* **2022**, *13*. [[CrossRef](#)]
36. Yin, Y.; Rioux, R.M.; Erdonmez, C.K.; Hughes, S.; Somorjai, G.A.; Alivisatos, A.P. Formation of hollow nanocrystals through the nanoscale Kirkendall effect. *Science* **2004**, *304*, 711–714. [[CrossRef](#)]
37. Wang, C.M.; Baer, D.R.; Thomas, L.E.; Amonette, J.E.; Antony, J.; Qiang, Y.; Duscher, G. Void formation during early stages of passivation: Initial oxidation of iron nanoparticles at room temperature. *J. Appl. Phys.* **2005**, *98*, 094308. [[CrossRef](#)]

38. Chernavskii, P.A.; Pankina, G.V.; Zaikovskii, V.I.; Peskov, N.V.; Afanasiev, P. Formation of hollow spheres upon oxidation of supported cobalt nanoparticles. *J. Phys. Chem. C* **2008**, *112*, 9573–9578. [[CrossRef](#)]
39. Srikala, D.; Singh, V.N.; Banerjee, A.; Mehta, B.R.; Patnaik, S. Control of magnetism in cobalt nanoparticles by oxygen passivation. *J. Phys. Chem. C* **2008**, *112*, 13882–13885. [[CrossRef](#)]
40. Srivastava, A.K.; Madhavi, S.; Menon, M.; Ramanujan, R.V. Synthesis of Co/Co₃O₄ Nanocomposite Particles Relevant to Magnetic Field Processing. *J. Nanosci. Nanotechnol.* **2010**, *10*, 6580–6585. [[CrossRef](#)]
41. Guo, B.; Xu, Y.; Zhou, S. Morphology dependence of low temperatures exchange bias Co/CoO core-shell nanoparticles/spheres by eco-friendly solvothermal route. *AIP Adv.* **2018**, *8*, 115115. [[CrossRef](#)]
42. Xie, X.; Ni, C.; Lin, Z.; Wu, D.; Sun, X.; Zhang, Y.; Wang, B.; Du, W. Phase and morphology evolution of high dielectric CoO/Co₃O₄ particles with Co₃O₄ nanoneedles on surface for excellent microwave absorption application. *Chem. Eng. J.* **2020**, *396*, 125205. [[CrossRef](#)]